Journal of Renewable and Sustainable Energy

Assessment of solar PV power potential over Asia Pacific region with remote sensing considering meteorological factors

Cite as: J. Renewable Sustainable Energy **11**, 013502 (2019); https://doi.org/10.1063/1.5059335
Submitted: 20 September 2018 . Accepted: 24 December 2018 . Published Online: 14 January 2019

Jeark Principe, and Wataru Takeuchi

Assessment of solar PV power potential over Asia Pacific region with remote sensing considering meteorological factors

Cite as: J. Renewable Sustainable Energy **11**, 013502 (2019); doi: 10.1063/1.5059335
Submitted: 20 September 2018 · Accepted: 24 December 2018 · Published Online: 14 January 2019

View Online Export Citation CrossMark

Jeark Principe[1,2,a)] and Wataru Takeuchi[1]

AFFILIATIONS

[1] Institute of Industrial Science, The University of Tokyo, Meguro-ku, Tokyo 153-8505, Japan
[2] Department of Geodetic Engineering, University of the Philippines Diliman, Quezon City 1101, Philippines

[a)] Author to whom correspondence should be addressed: japrince@iis.u-tokyo.ac.jp. Tel.: +81-03-5452-6409. Fax: +81-03-5452-6410

ABSTRACT

The intensity of solar radiation (SR) is one of the most important required inputs for the estimation of photovoltaic (PV) power station output. Meanwhile, the efficiency of solar PV systems is affected by meteorological factors such as temperature, dust, precipitation, and snow. Meteorological data from satellites provide a viable way for estimating PV potential due to its advantage in spatial coverage and temporal resolution. This paper presents a new approach to adjust SR data from satellites based on the cloud optical thickness (CLOT) before evaluating the solar PV power (P_{PV}) potential, with the effective efficiency of solar cells computed based on temperature, dust, precipitation, and snow. The objective of this study is to evaluate the over-all spatiotemporal solar PV potential in the Asia Pacific region which will holistically include limiting meteorological factors and identify which factor contributes most significantly to the decrease in solar PV potential in selected cities in the region. First, SR and CLOT data from Advanced Himawari Imager 8 and a SKYNET station were processed to derive the correction factor for solar radiation data. Second, satellite data for temperature (MOD11), precipitation (global satellite mapping of precipitation), dust (MOD04), and snow cover (MOD10) were processed to derive the effective solar PV efficiency. Finally, maps showing the seasonal PV power potential over the Asia Pacific region were generated, with selected cities zoomed in for detailed analysis using mean monthly values from March 2016 to February 2017. The results showed that the maximum theoretical P_{PV} in the region was estimated to be 1.9 GW per 17.5 km^2 effective pixel area. Moreover, P_{PV} decreased by maximum values of 180 MW, 550 MW, and 225 MW due to temperature, dust, and snow, respectively. For Beijing, Tokyo, and Jakarta, the major contributor to the decrease in P_{PV} is dust, while Khabarovsk is consistently affected by snow effects. Initial validation of the model shows over- and underestimation of solar PV output compared to the actual values by as high as 30%. However, very high values of coefficient of determination (>0.90) show promising results of the model. The contribution of this study is two-fold: regional-scale assessment of P_{PV} potential and investigation of the collective effect and individual contributions of dust, temperature, and snow to the decrease in P_{PV} potential.

NOMENCLATURE

Variables

A_{cell} total aggregated pixel area allocated for the installation of solar PV panels
Dust_Decr contribution of dust to the decrease in theoretical solar PV power
E_{gen} equivalent generated output energy in kWh
LST_Decr contribution of temperature to the decrease in theoretical solar PV power
P_{PV} solar photovoltaic power
P'_{PV} total effective solar photovoltaic power output
$P'_{PV,X}$ effective solar PV power output considering X individual meteorological factors
R' adjusted solar radiation data from AHI8
sc snow cover

Snow_Decr	contribution of snow to the decrease in theoretical solar PV power
V_P and V_M	predicted (estimated) and measured (actual) values, respectively
x_d and x_r	variables for dust masking using AOD and precipitation rate values, respectively
$\Delta\eta_t$, $\Delta\eta_d$, and $\Delta\eta_s$	decrease in solar cell efficiency due to temperature, dust, and snow, respectively
η	conversion efficiency of the solar cell

Acronyms

AHI	Advanced Himawari Imager
AOD	Aerosol Optical Depth
APR	Asia Pacific Region
CLOT	Cloud Optical Thickness
EPA	Effective Pixel Area
GSMaP	Global Satellite Mapping of Precipitation
JAXA	Japan Aerospace Exploration Agency
LST	Land Surface Temperature
MFG	Meteosat First Generation
MODIS	Moderate Resolution Imaging Spectroradiometer
MOD04	MODIS Aerosol Product
MOD10	MODIS Snow Cover Product
MOD11	MODIS Land Surface Temperature and Emissivity Product
NOCT	Nominal Operative Cell Temperature
PPE	Percentage Prediction Error
SKYNET	An observation network dedicated for aerosol-cloud-radiation interaction research studies
SRTM	Shuttle Radar Topography Mission
SWR	Shortwave Radiation
TSH	Total Sunshine Hours
TSPA	Total Solar Panel Area (used in the actual installation)

Units

kWh	kilowatt-hour, a unit of energy
MW	megawatts, a unit of power

I. INTRODUCTION

Energy is an indisputable necessity for the modern society. As the world's population increases, the demand for energy also rises since the population growth rate is recognized as an important driver of energy (US EIA, 2017) to ensure a better life environment and technological and economic development (Sampaio and Gonzalez, 2017). However, the annual total greenhouse gas (GHG) emissions from the global energy supply sector continue to increase as well. It was reported that the combustion of fossil fuels continues to dominate the global energy market that is striving to meet the ever-increasing demand for heat, electricity, and transport fuels (Sims *et al.*, 2007). In Asia alone, the reliance on fossil fuels is 86% in the energy mix which is 5% higher than the global average in 2014 (AIIB, 2017). For sustainable development, however, there is a need for an efficient way of extracting energy from renewable sources. One such alternative is solar—a low carbon resource with both scalability and technological maturity to meet the fast-growing global demand for electricity (Chander *et al.*, 2015). Solar photovoltaic (PV) contributed to an annual market increase in about 50%, making it the world's leading source of additional power generating capacity of at least 75 GW in 2016 (REN21, 2017).

Meteorological data from satellites provide a viable way for estimating the PV potential due to its advantage in spatial coverage and temporal resolution. For instance, the SolarGIS database that was used to determine the potential of selected renewable energy sources in the Greater Mekong Subregion contains irradiance values in the 30-min time-step calculated from the Meteosat first generation (MFG) satellite and elevation from Shuttle Radar Topography Mission (SRTM) (ADB, 2015). Moreover, Higurashi and Nakajima (1999) acknowledged that the use of data from satellites was very effective while performing a large-scale study of aerosol optical properties.

The theoretical solar PV potential is not reached due to several limiting meteorological factors including the effects of dust, temperature, precipitation, snow, and clouds. Both the increase in temperature (Menes-Rodrìguez *et al.*, 2005) and dust deposition (Goossens *et al.*, 1993) contribute to the decrease in the PV solar efficiency. Meanwhile, insolation is directly related to the cloud cover (Kim *et al.*, 2017). Moreover, it has also been observed that the snow cover reduces the overall performance of solar modules mounted at different tilt angles (NAIT, 2016). The objective of this study is to evaluate the over-all spatiotemporal solar PV potential in the Asia Pacific region (APR) using remote sensing that will holistically include such limiting factors and identify which contributes most significantly to the decrease in the solar PV potential in selected cities in the region. The approach used in this study utilized various remote sensing satellite products for solar radiation, cloud optical thickness (CLOT), land surface temperature (LST), precipitation, dust, and snow.

Previous studies on solar PV power potential investigated the effects of the above-mentioned meteorological factors separately and their methods applied in local settings or very small areas. For instance, such experiments were done on the roof of a building (Paudyal and Shree, 2016 and NAIT, 2016) and in a laboratory environment under controlled conditions (Beattie *et al.*, 2012; Chander *et al.*, 2015; El-Shobokshy and Hussein, 1993; and Goossens *et al.*, 1993). As such, this study contributes to the body of knowledge by providing a method for regional-scale assessment of P_{PV} potential and investigating the collective effect and individual contributions of dust, temperature, and snow to the decrease in P_{PV} potential.

II. METHODOLOGY

A. Data description

Derived products from Advanced Himawari Imager 8 (AHI8) are downloaded via the Japan Aerospace Exploration Agency (JAXA) Himawari Monitor (eorc.jaxa.jp/ptree/index.html). These two products are the Shortwave Radiation (SWR) and the Cloud Property (CLOT) both at spatial and temporal resolutions of 5 km and 10 min, respectively. The daily Aerosol Optical Depth (AOD) from the MODIS aerosol product (MOD04 L2) at a resolution of 10 km was used to extract dust information (Levy et al., 2013). For LST data, the MODIS Land Surface Temperature and the Emissivity 8-day global product (MOD11 L3) at a resolution of 1 km were used (Wan, 1999). To extract precipitation rate data, the daily average rainfall estimates from global satellite mapping of precipitation (GSMaP) at a resolution of 0.1° × 0.1° were used (Okamoto et al., 2005). Finally, the monthly snow cover was extracted from the monthly Global 0.05° CMG (version 6) MOD10 L3 dataset (Hall et al., 2001). The period analyzed for this study is one complete year, starting from March 2016 to February 2017 since the SWR data from AHI8 are only available from March 2016. The seasons defined in this study were MAM (March to May), JJA (June to August), SON (September to November), and DJF (December to February).

B. Methods

The general methodology adopted in this study is shown in Fig. 1. First, the SWR data from AHI8 were adjusted to generate R'. The adjustment process entailed the use of CLOT data to fit the original SWR data with the ground data observations (http://atmos2.cr.chiba-u.jp/skynet/chiba/chiba.html) and derive the correction factor for solar radiation data (CFSR) via a non-linear regression technique by Principe and Takeuchi (2018). SWR data were then adjusted using CFSR to generate R'. The technique of adjusting the solar radiation values derived from AHI-8 using CLOT data worked well during the summer and winter seasons since R' has a smaller absolute difference to the SKYNET data (Table I). It performed unsatisfactorily, however, during spring and autumn seasons when, most probably, the cloud cover is not a major factor affecting SWR. Nonetheless, the technique's effectiveness to adjust the solar radiation values during the summer (JJA) is worth noting since the peak of solar intensity is expected and the discrepancy between the ground- and satellite-based values is at a maximum during this season compared to other seasons of the year.

1. Computation of solar PV power output and decrease in solar cell efficiency

The theoretical solar PV power (P_{PV}) output in megawatts (MW) is computed using Eq. (1), where A_{cell} is the total aggregated pixel area allocated for the installation of solar PV panels, η is the conversion efficiency of the solar cell, and R' is the adjusted solar radiation data from AHI8

$$P_{PV} = A_{cell}\,\eta\,R'. \tag{1}$$

Equation (1) is adapted from the original model equation in the study by Liu et al. (2017) where the modifications include the merging of two separate variables for the number of PV cells (N) and the area of a single PV cell (S_A) to a single variable A_{cell}. Moreover, in Eq. (1), we considered the adjusted solar radiation (R') instead of the actual intensity of solar radiation (R_T) since this study did not use the ground-observed values of solar radiation but used instead the satellite-derived values as adjusted to fit with the actual ground data.

The decrease in solar cell efficiency due to temperature ($\Delta\eta_t$), dust ($\Delta\eta_d$), and snow ($\Delta\eta_s$) is computed using Eqs. (2), (3), and (4), respectively. The over-bar in these equations indicates the computation of mean values over the evaluation period. $\Delta\eta_t$ is computed using the typical nominal operative cell temperature (NOCT) with $NOCT_{max}$ set at 45 °C and the temperature coefficient of efficiency ($d\eta/dT = 0.094$) (Chander et al., 2015) at every $\boldsymbol{i}$th day for each season with $\boldsymbol{n}$ being the total number of days

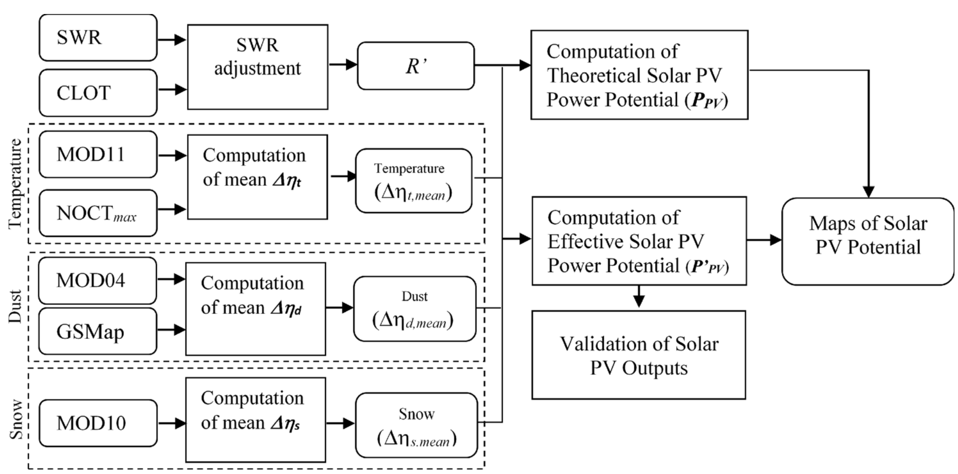

FIG. 1. The general methodology used in this study. The theoretical solar PV power potential (P_{PV}) was derived using the adjusted shortwave radiation (SWR). The effect of temperature ($\Delta\eta_t$) was derived using the LST product from MOD11, while the effect of dust ($\Delta\eta_d$) was derived from a binary technique considering rainfall (cleaning agent) and non-rainfall (the dust effect is not eliminated) events using GSMaP rainfall rate data and AOD data (representing dust) from MOD04. Moreover, the effect of snow ($\Delta\eta_s$) was derived from snow cover percentage data of MOD10. Such effects of meteorological factors on the efficiency of solar PV cells were then used to compute for the effective solar PV power potential (P'_{PV}). The computed P'_{PV} was in turn validated against the outputs from actual solar PV installations. Finally, maps of solar PV potential were generated.

TABLE I. Absolute differences in solar radiation between SKYNET and AHI8 original (AHI8) and adjusted (AHI8Cor) SWR data.

	Absolute difference in solar radiation (W/m^2)	
Season	AHI8—SKYNET	AHI8Cor—SKYNET
Spring	21.29	30.87
Summer	61.99	15.85
Autumn	12.69	42.56
Winter	9.80	7.85

$$\overline{\Delta\eta_t} = 0.094\frac{\sum_{i=1}^{n} \mathrm{LST} - \mathrm{NOCT_{max}}}{n}. \tag{2}$$

$\Delta\eta_d$ is computed using Eq. (3) where the constant 0.3 is the reported decrease in solar cell efficiency due to dust by Sayigh (1978). x_d is either 0 (AOD $\leq$ 0) or 1 (AOD > 0) for the non-dust or dust day, respectively. x_r is either 1 or 0 for the no rain or rainy day, respectively. This approach therefore considers the cleaning effect of rain on solar panels and cancels the effect of dust on days with rainfall (i.e., when $x_d = 1$ and $x_r = 0$).

$$\overline{\Delta\eta_d} = 0.3\frac{\sum_{i=1}^{n} x_{d_i} x_{r_i}}{n}. \tag{3}$$

$\Delta\eta_s$ is computed using the snow cover (sc) from MOD10 (values are 0–100) assuming a snow coefficient of efficiency ($d\eta/ds$ = 0.16) (NAIT, 2016) at every $\boldsymbol{i}$th month for each season with $\boldsymbol{n}$ being the total number of months

$$\overline{\Delta\eta_s} = 0.0016\frac{\sum_{i=1}^{n} sc_i}{n}. \tag{4}$$

The effective solar PV power output considering the individual meteorological factors ($P'_{PV,X}$) in MW was computed as

$$P'_{PV,X} = A_{cell}\,\eta\, R'(1 - \overline{\Delta\eta_X}), \tag{5}$$

where subscript X denotes the meteorological components (e.g., d = dust, s = snow, and t = temperature).

The total effective solar photovoltaic power output (P'_{PV}) in MW was computed as

$$P'_{PV} = A_{cell}\,\eta\, R'(1 - \overline{\Delta\eta_t} - \overline{\Delta\eta_d} - \overline{\Delta\eta_s}). \tag{6}$$

In this study, the final spatial resolution of the raster data used was 5 km and it was assumed that only 70% of the pixel area will be utilized for solar PV installation with a PV cell efficiency of 13% (for thin-film cells) according to Sampaio and Gonzalez (2017). The type of solar cell based on thin film silicon was selected since it offers a promising value of significantly lowering the costs of producing energy from solar PV, thereby attracting future investors and users of this technology (Chen and Sopori, 1999).

2. Comparison of computed solar PV power with actual reported outputs

The computed seasonal solar PV power was compared with the actual generated PV output data from the installations published in the website of PVOutput.org (https://pvoutput.org). The website offers a free service platform to share, compare, and monitor live solar photovoltaic (PV) and energy consumption data (PVOutput.org, 2018). Since the reported actual outputs were in energy units (kWh), the computed P'_{PV} in MW must be converted to kWh using the following equation:

$$E_{gen}(\mathrm{kWh}) = P'_{PV} \times TSH \times TSPA \times 1000/EPA, \tag{7}$$

where E_{gen} is the equivalent generated output energy in kWh; P'_{PV} is the total effective solar photovoltaic power output in MW; *TSH* is the average total sunshine hours; *TSPA* is the total solar panel area used in the actual installation in m^2; and *EPA* is the effective pixel area (for this study, EPA = 5000 m × 5000 m × 0.7 = 1.75×10^7 m^2 or 17.5 km^2).

The description of the two solar PV installations used in this study for validation purposes is shown in Table II. Only this limited number of actual solar PV systems was used because there were only a few installations in the Asia Pacific region with data in PVOutput.org and most of them did not have data for periods covered in this study. Meanwhile, the TSH data were obtained from different sources including the Australian Government Bureau of Meteorology for Signal Hill (2005), and the Thai Meteorological Department for Bangkok Soladin (2014).

The estimated values of solar PV output were assessed using the percentage prediction error (PPE) as given by Kim *et al.* (2017) in the following equation:

$$\mathrm{PPE} = \frac{|V_P - V_M| \times 100}{V_M}, \tag{8}$$

where V_P and V_M are the predicted (estimated) and measured (actual) values, respectively. Equation (8) implies that the lower the value for PPE is the better the estimation is.

III. RESULTS AND DISCUSSION

Satellite data were processed to produce three sets of PV solar potential products for the Asia Pacific region: theoretical, effective (considering individual meteorological factors), and

TABLE II. Actual solar PV installations in PVOutput.org used in this study for validation.

Name	Location	System size (kW)	Number of panels	Orientation	Tilt (deg)
Signal Hill	Perth, Australia	3.36	16	NE	18
Bangkok Soladin	Bangkok, Thailand	0.65	5	S	15

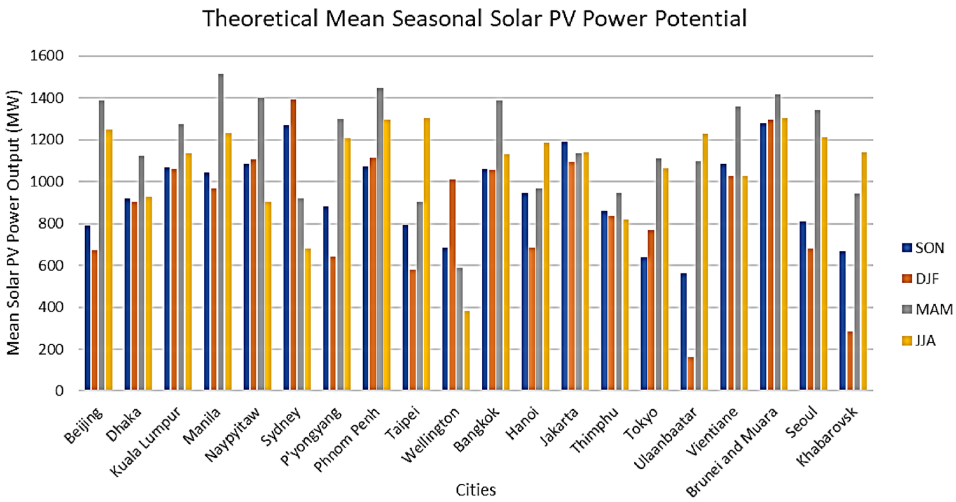

FIG. 2. Theoretical mean seasonal solar PV power output for selected cities in the Asia Pacific region.

total effective. Moreover, zoomed in analysis for selected cities in the region was performed to determine which among the factors are significantly affecting the PV solar potential. The equivalent generated output energy (E_{gen}) is also compared with the actual output of solar PV installations in two locations within the Asia Pacific region. Finally, the limitations and possible sources of error of the technique used in this study for the estimation of P_{PV} are also presented.

A. Theoretical solar PV power potential

The satellite-derived mean theoretical seasonal solar photovoltaic output power maps for the Asia Pacific Region are generated using Eq. (1). Meanwhile, Fig. 2 shows the solar PV power output in selected cities in the Asia Pacific region. Among these 20 cities examined, Brunei and Muara, Sydney, Manila, and Taipei, have the highest estimated solar PV power during SON (1204.73 MW), DJF (1487.3 MW), MAM (1473.57 MW), and JJA (1243.94 MW) seasons, respectively.

The corresponding spatial distribution maps in the Asia Pacific region during the different seasons are shown in Fig. 3. The theoretical solar PV potential is high during the JJA season in most of the region, except in Southern Australia and mountainous areas in India, Nepal, Myanmar, and Bhutan. Since A_{cell} and η are assigned with fixed values, the variation of P_{PV} is solely dependent on R' the value of which varies according to the surface topology, zenith angle, atmospheric gases, and clouds, among others (Gokmen *et al.*, 2016; Lee *et al.*, 2018; Gupta *et al.*, 2016; and Frouin and Murakami). Since the effects of clouds and the clear atmosphere were already accounted in the algorithm to estimate SWR from AHI8 (Frouin and Murakami, 2007), topographic shading and short sunshine hours (in the case of Australia) are possible reasons for the low P_{PV} potential during the said season. Meanwhile, Australia has very high potential during DJF and SON with a potential of about 1.6 GW for both seasons, the highest among the Asia Pacific countries. Australia experiences an average sunshine hour of up to 11 h during these seasons (Australian Government Bureau of Meteorology, 2005) which translates to more solar irradiance available for solar energy conversion by PV systems.

B. Decrease in solar PV power potential due to temperature

The satellite-derived seasonal decrease in solar photovoltaic output power due to temperature for the Asia Pacific Region was generated using Eqs. (1), (2), and (5). The corresponding spatial distribution maps during the different seasons are shown in Fig. 4. The maximum decrease in P_{PV} was 180 MW, about 9.4% of the theoretical potential. During the DJF season, most of the area in Australia experiences a decrease in solar PV potential due to the high temperature, with some portions in the northwest area affected during the MAM season. It can also be observed from Fig. 4 that during the JJA season, areas in northern China and southern Mongolia in the Gobi Desert have a notable decrease in solar PV potential. The reason was that in these areas, LST can reach up to 50 °C during the summer season. Some parts of India, Thailand, Myanmar, and Cambodia experience a decrease in P_{PV} potential during the MAM season.

As can be seen in Fig. 4, the effect of the temperature on solar PV performance was very negligible in many parts of the region. This can be attributed to the use of LST to estimate the actual temperature of the solar cells (T_{cell}). Thermal radiance coming from the land surface is retrieved by the satellites which are then used to estimate LST on the theoretical basis that the total radiance emitted by the ground increases rapidly with temperature (Mildrexler *et al.*, 2011). As such, the direct use of LST in place of T_{cell} may result in an error in the estimation of temperature effects on P_{PV} potential. LST was used in this study since actual long-term T_{cell} data were not available for the whole Asia Pacific Region. For future work, the conversion of LST to T_{cell} can be done by first linking the LST to air temperature (T_{air}) and T_{air} to T_{cell} following the studies of Li *et al.* (2008), Jin and Dickinson (2010), Mildrexler *et al.* (2011), and Gokmen *et al.* (2016). Finally, wind can also affect P_{PV}

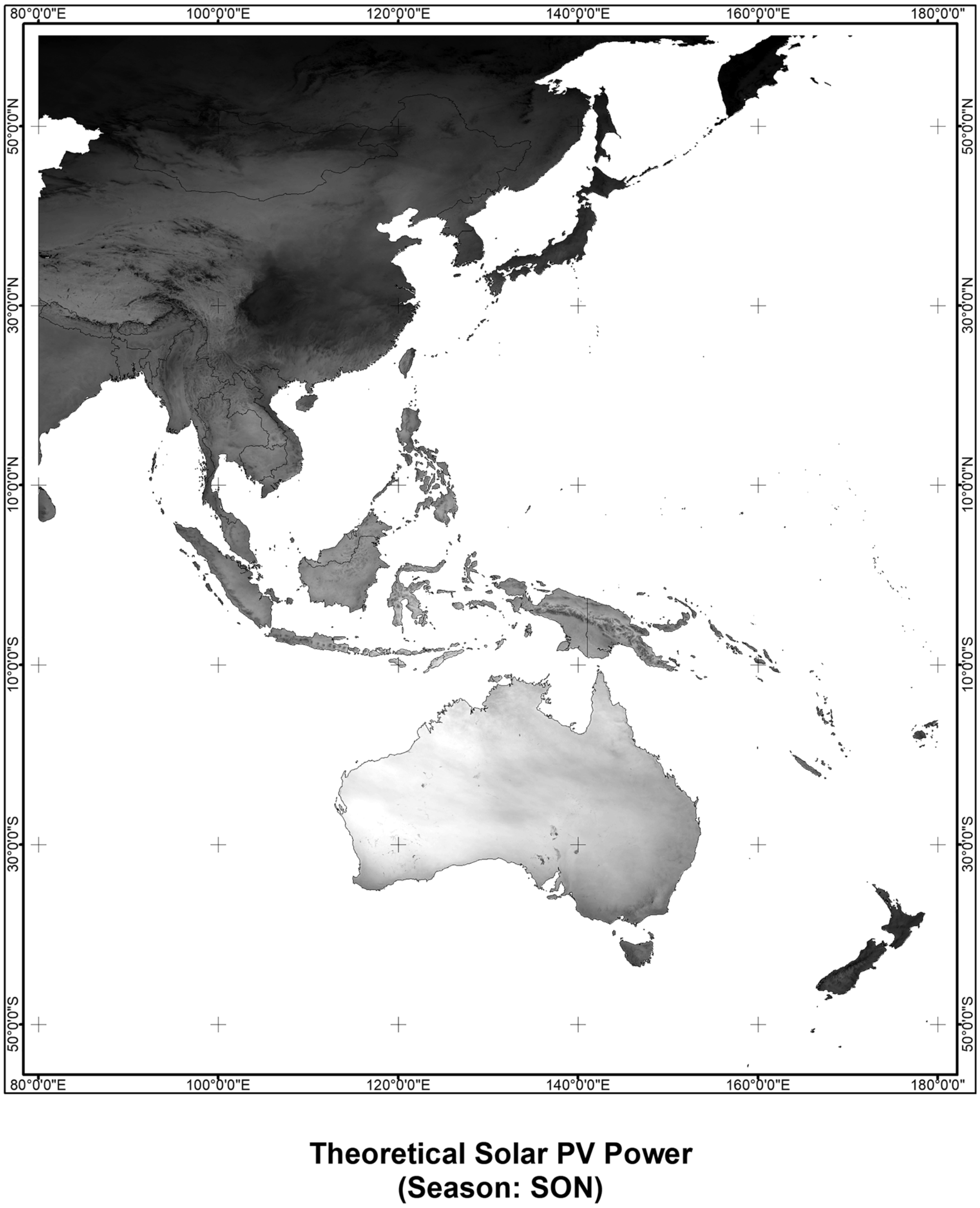

FIG. 3. Theoretical mean seasonal solar PV power (in megawatts) in the Asia Pacific region: (a) DJF; (b) MAM; (c) JJA; and (d) SON.

potential in terms of its cooling effect on PV systems (Gokmen et al., 2016). In the current model, the effect of temperature seemed to be very negligible, but if T_{cell} is used instead of LST, it is expected to get very high temperature values which will degrade the solar cell efficiency down to 0. As such, wind speed will be considered in the future model update. Rainfall may also help in cooling down solar panels, but the solar-driven rainwater cooling device is not efficient and cost-effective especially for solar PV installations for domestic houses (Wu and Xiong, 2014). For this reason, rainfall was not considered as a cooling agent for solar PV systems.

C. Decrease in solar PV power potential due to dust

Using Eqs. (1), (3), and (5), maps for the satellite-derived seasonal decrease in solar photovoltaic output power due to dust for the Asia Pacific Region were generated. The corresponding spatial distribution maps during the different seasons are shown

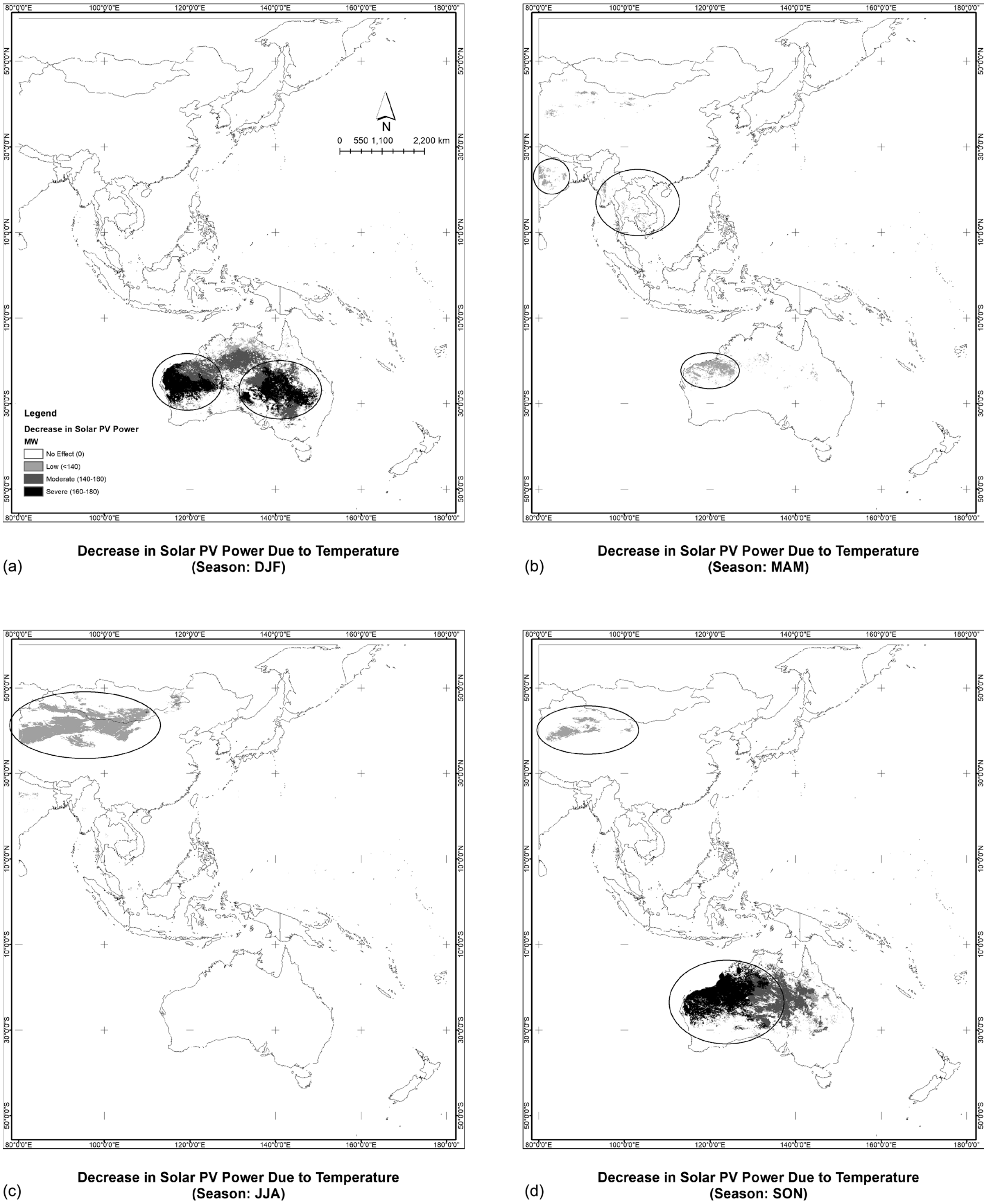

FIG. 4. Decrease in mean seasonal solar PV power (in megawatts) due to temperature in the Asia Pacific region: (a) DJF; (b) MAM; (c) JJA; and (d) SON. The areas in circles are where the temperature has a relatively high impact on the decrease in solar PV output compared to other areas in the region for that season.

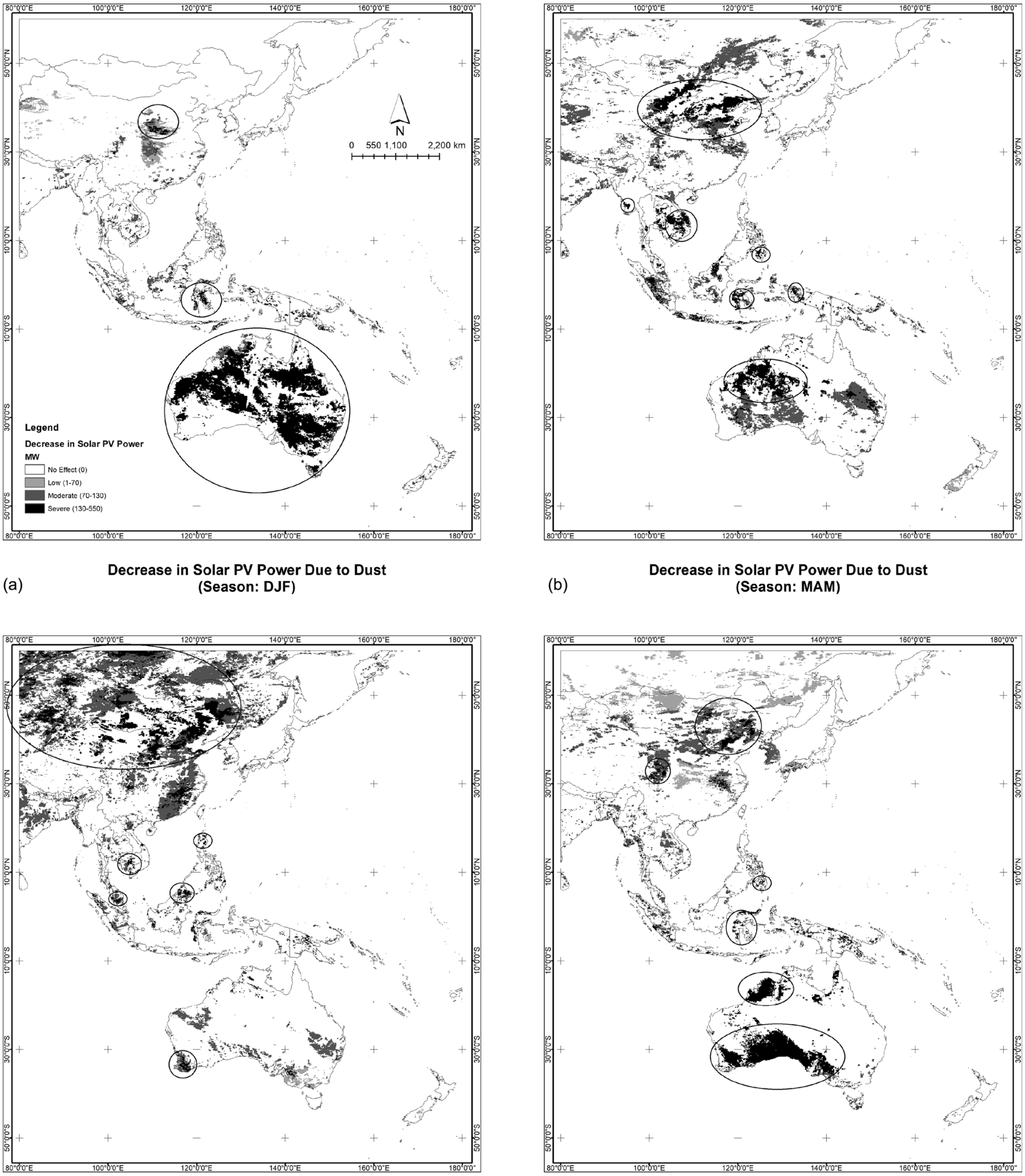

(a) **Decrease in Solar PV Power Due to Dust (Season: DJF)**

(b) **Decrease in Solar PV Power Due to Dust (Season: MAM)**

(c) **Decrease in Solar PV Power Due to Dust (Season: JJA)**

(d) **Decrease in Solar PV Power Due to Dust (Season: SON)**

FIG. 5. Decrease in mean seasonal solar PV power (in megawatts) due to dust in the Asia Pacific region: (a) DJF; (b) MAM; (c) JJA; and (d) SON. The areas in circles are where dust have a relatively high impact on the decrease in solar PV output compared to other areas in the region.

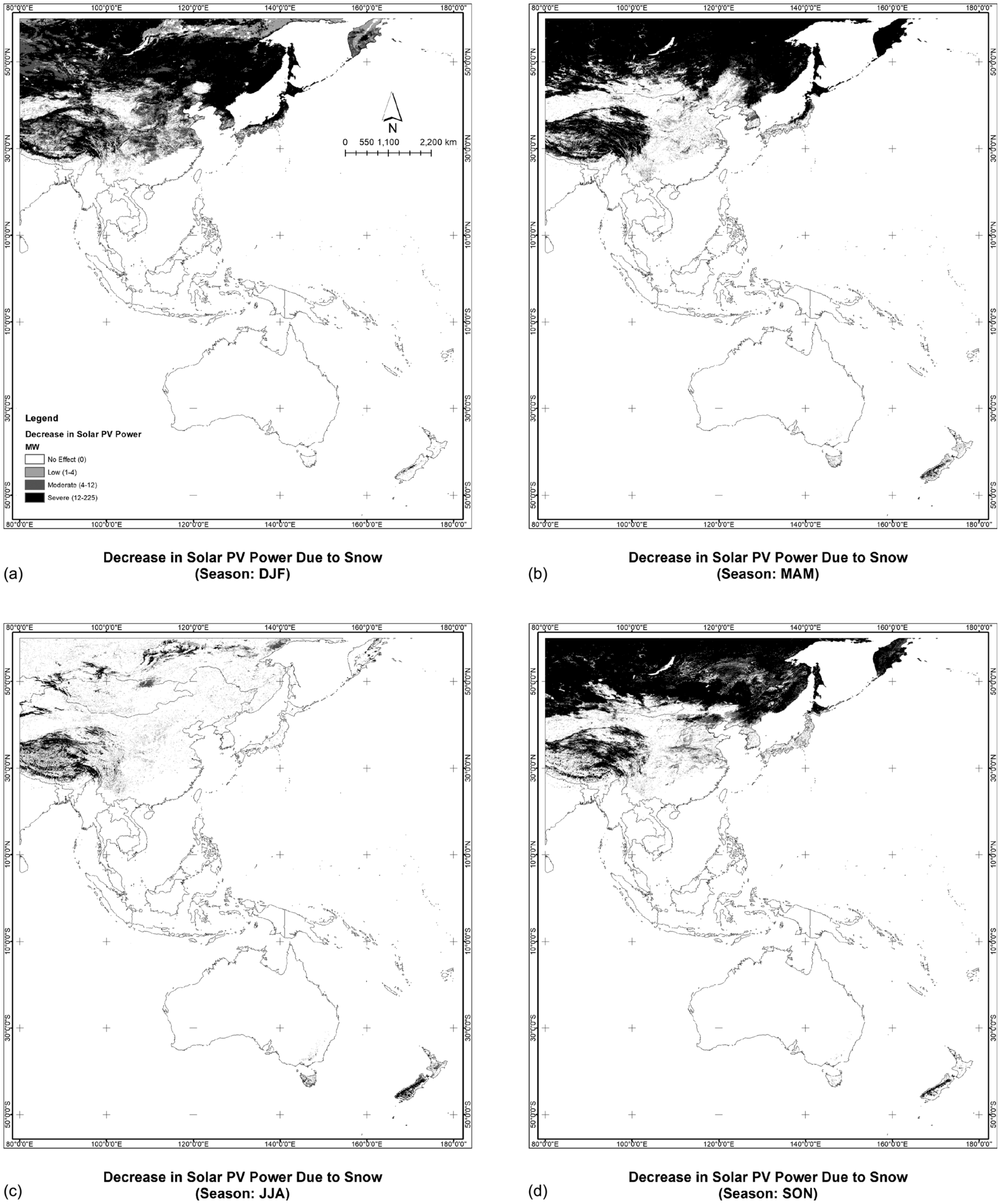

FIG. 6. Decrease in mean seasonal solar PV power (in megawatts) due to snow in the Asia Pacific region: (a) DJF; (b) MAM; (c) JJA; and (d) SON. The areas in the latitudes above ∼30°N and below ∼30°S are where snow have an impact on the decrease in solar PV output.

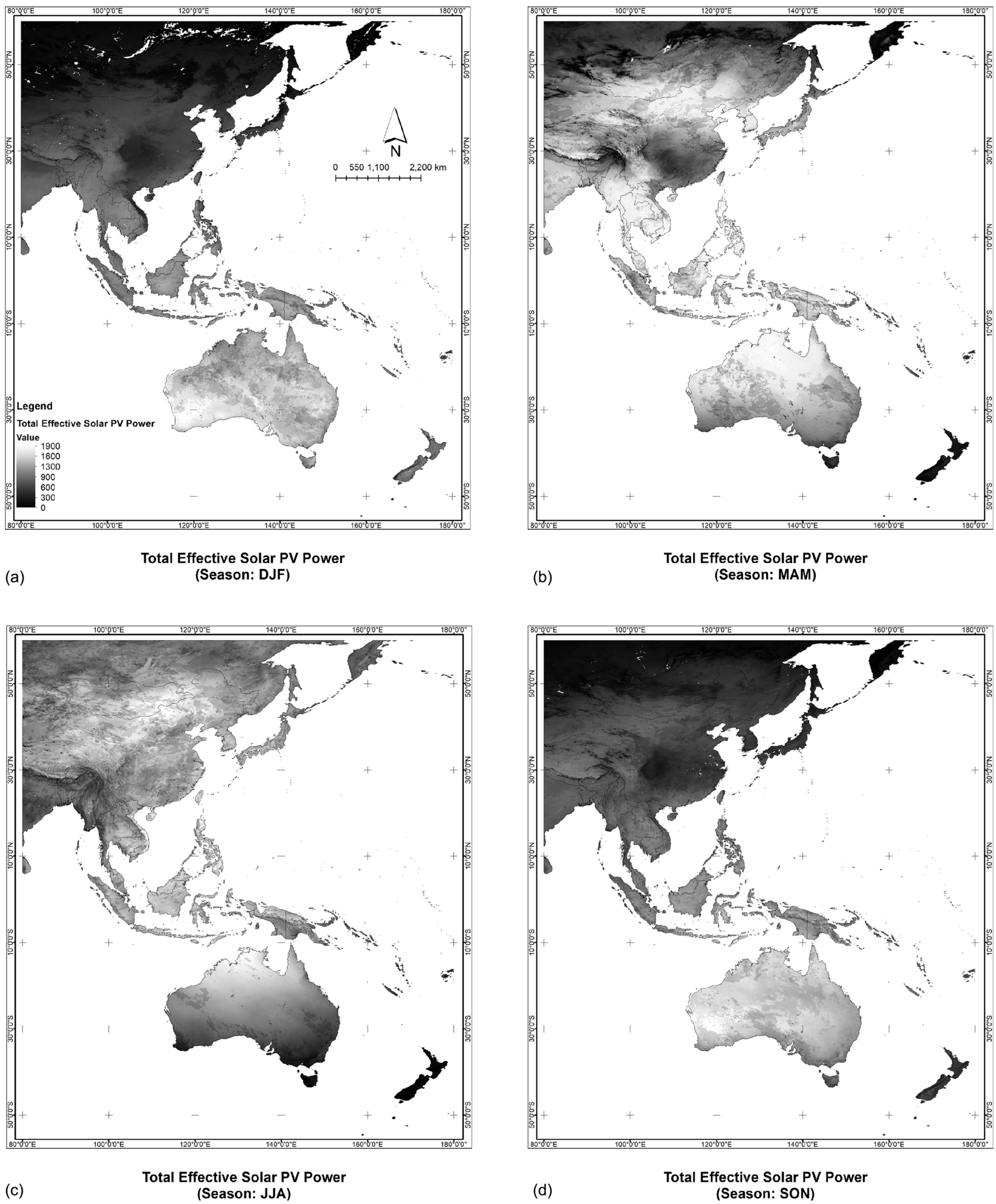

FIG. 7. Total effective mean seasonal solar PV power (in megawatts) in the Asia Pacific region: (a) DJF; (b) MAM; (c) JJA; and (d) SON.

in Fig. 5 which reveals that almost all countries in the region suffer from the effects of dust. The effects are severe in East Asia (except in Japan and Korea) during the JJA season. Australia is consistently affected by dust especially during DJF and MAM seasons. The southern part of Australia also experienced severe effects from dust during the SON season. Finally, the maximum decrease in solar PV power potential due to dust was 550 MW. It seems that the precipitation rate in the region is not enough to serve as a cleaning agent for solar cell installations. Manual scheduled cleaning of the solar PV systems is therefore suggested for these areas.

The interaction between rainfall and dust affects the output power of solar cells. Depending on its intensity, rainfall can either promote or impede the accumulation of dusts on a PV module. Kimber *et al.* (2006) suggested a minimum of 20 mm/day of rain to clean a PV system from dusts. Meanwhile, even the size of dust particles affects PV power output. Dust of finer particles is distributed in a more uniform manner than that for the coarser ones, thus minimizing the voids between particles through which light can pass (El-Shohokshy and Hussein, 1993). Such dust and rainfall characterization will therefore be considered in updating the current model.

D. Decrease in solar PV power potential due to snow

Using Eqs. (1), (4), and (5), maps for the satellite-derived seasonal decrease in solar photovoltaic output power due to snow for the Asia Pacific Region were generated. The corresponding spatial distribution maps during the different seasons are shown in Fig. 6 which shows that areas with latitudes above $\sim$30°N and below $\sim$30°S were affected by this limiting factor. Areas in North East and North West China, Mongolia, Russia, Japan, and Korea were significantly affected compared to other areas in the region during DJF and MAM seasons. The same is true for New Zealand during JJA and SON seasons. The maximum decrease in the solar PV potential was computed at 225 MW, which is about 12% of the theoretical P_{PV} which is below the maximum snow effect set in the model (i.e., 16%). As such, there is a possible underestimation of snow effects. For future work, we plan to vary the threshold level to efficiently model the snow dynamics in the region.

For an optically thick layer, the Bouguer-Lambert law predicts an exponential decrease in solar irradiance with the depth (Perovich, 2007) which will yield lower P_{PV}. Due to its better spatial resolution and temporal coverage, the snow cover product from MODIS (MOD10) was used instead of the snow depth with the assumption that the two are highly correlated. However, in the model update, we plan to derive the snow depth from the snow water equivalent (SWE) product of the Advanced Microwave Scanning Radiometer for Earth Observing System (AMSR-E) (Chang and Rango, 2000).

E. Total effective solar PV power

Combining the effects of temperature, dust, and snow gives the total effective P_{PV} as facilitated by Eq. (6). Maps for the satellite-derived total effective seasonal solar photovoltaic output power for the Asia Pacific Region were generated and are shown in Fig. 7. Moreover, Fig. 8 shows the percent decrease in P_{PV} during different seasons at selected cities in APR. The cities of Ulaanbaatar (−12%), Khabarovsk (−16%), Dhaka (−9%), and Beijing (−13%) have the highest percentage decrease in P_{PV} during the SON, DJF, MAM, and JJA seasons, respectively.

As snow and temperature cannot be controlled, significant efforts should be devoted to reducing dust emission. Such a reduction in dust effects will result in a saving of at most 167 MW of energy during the JJA season in Beijing. This amount of energy can support about 6 families of 6 in China for a month based on the reported electric power consumption according to The World Bank (2014).

F. Effects of temperature, dust, and snow on the decrease in solar PV potential in selected cities in the Asia Pacific region

The cities of Beijing (China), Tokyo (Japan), Khabarovsk (Russia), and Jakarta (Indonesia) were selected to see the percent contribution of the three meteorological factors considered in

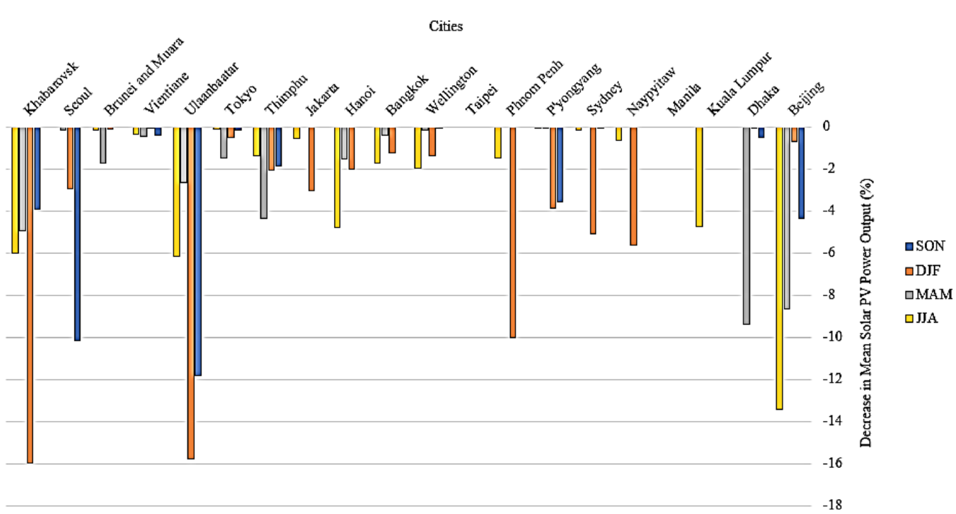

FIG. 8. Decrease in mean seasonal solar PV power potential for selected cities in the Asia Pacific region.

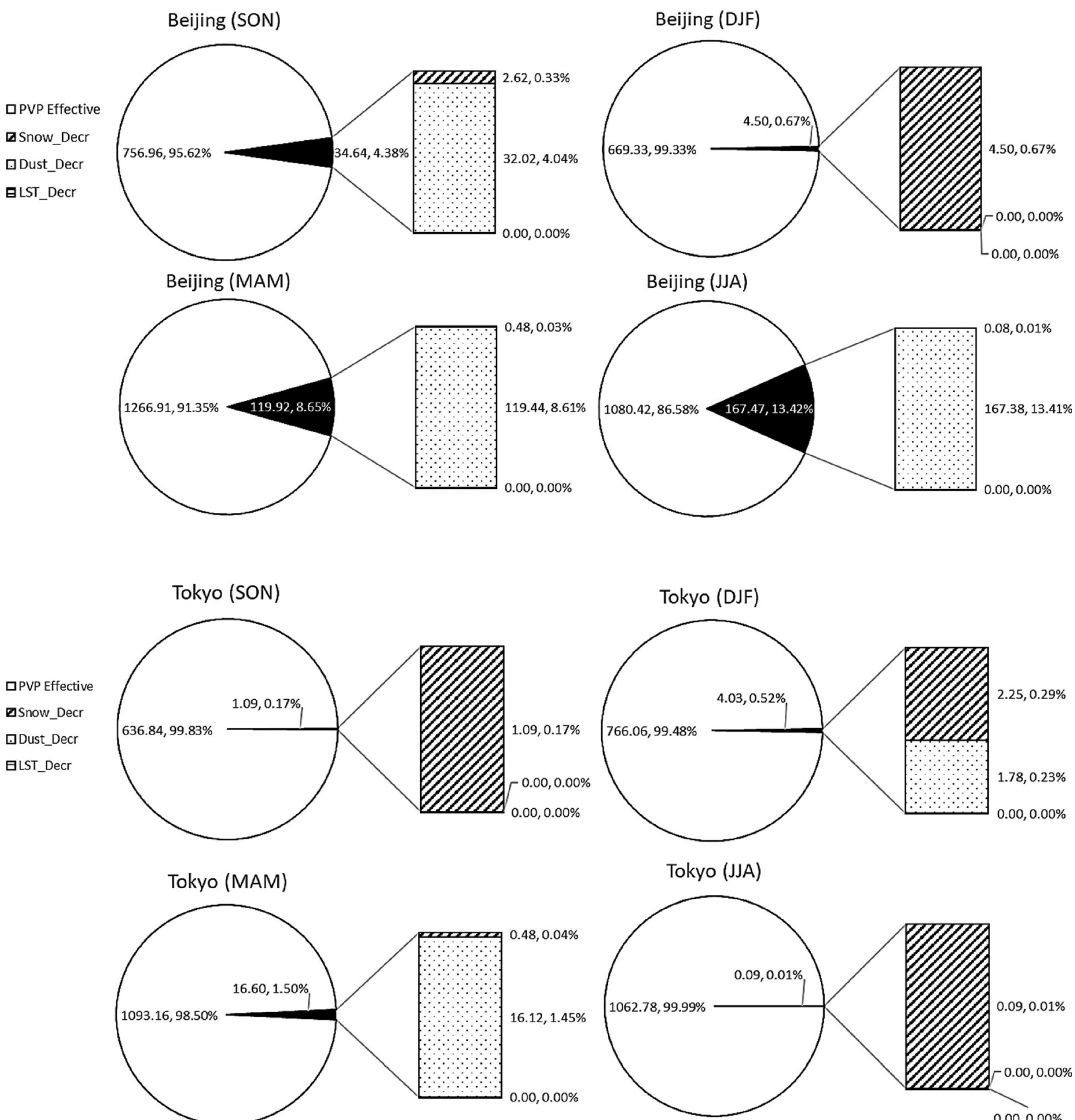

(b)

FIG. 9. Contribution of dust (Dust_Decr), snow (Snow_Decr), and temperature (LST_Decr) to the decrease in theoretical solar PV power (P_{PV}) in (a) Beijing and China, (b) Tokyo and Japan, (c) Khabarovsk and Russia, and (d) Jakarta and Indonesia. The first value in the data labels is the output power in MW, while the second is the percentage contribution to the total in %.

this study to the overall decrease in solar PV potential with respect to the theoretical values.

Figure 9(a) shows that in Beijing's case, dust is a major contributor to the decrease in $\mathbf{P_{PV}}$ for all seasons except in DJF where snow cover is the only factor affecting the said decrease. In Tokyo's case [Fig. 9(b)], the major contributor varies with the season. Snow is the major factor during SON; snow and dust have equal contributions during DJF; dust is the major

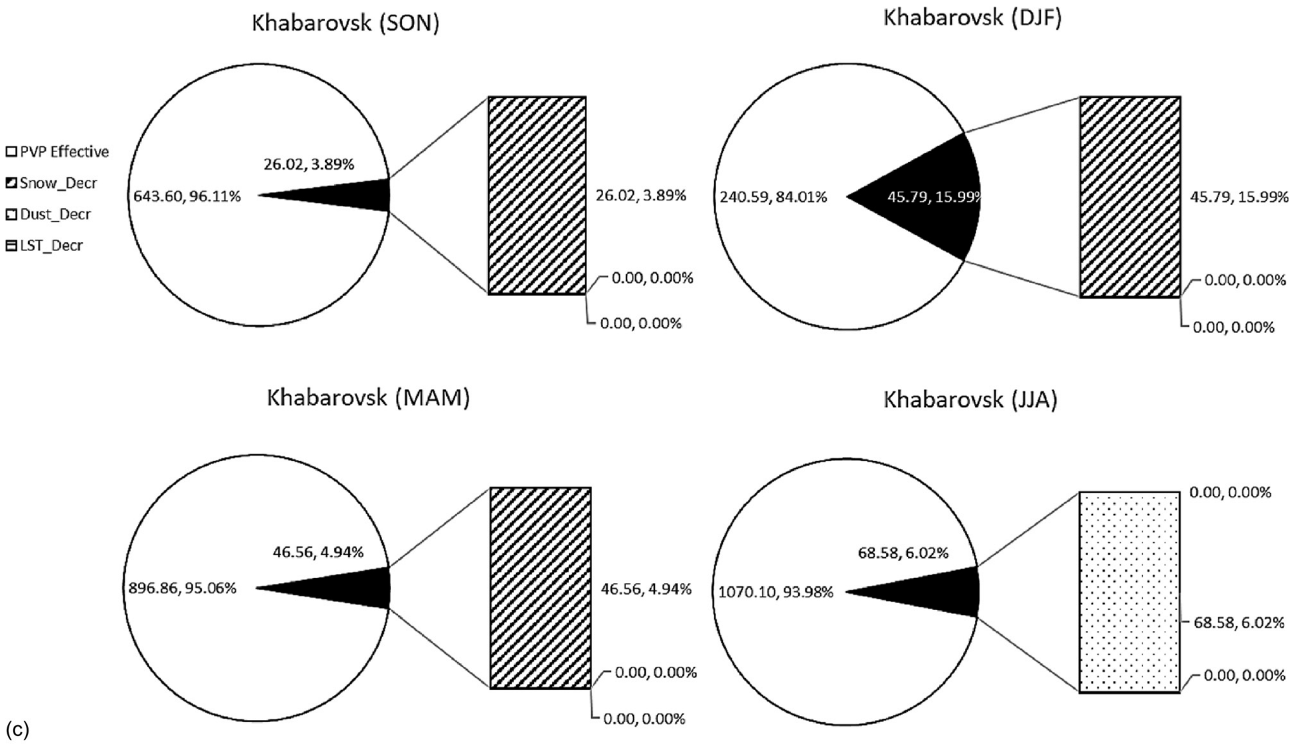

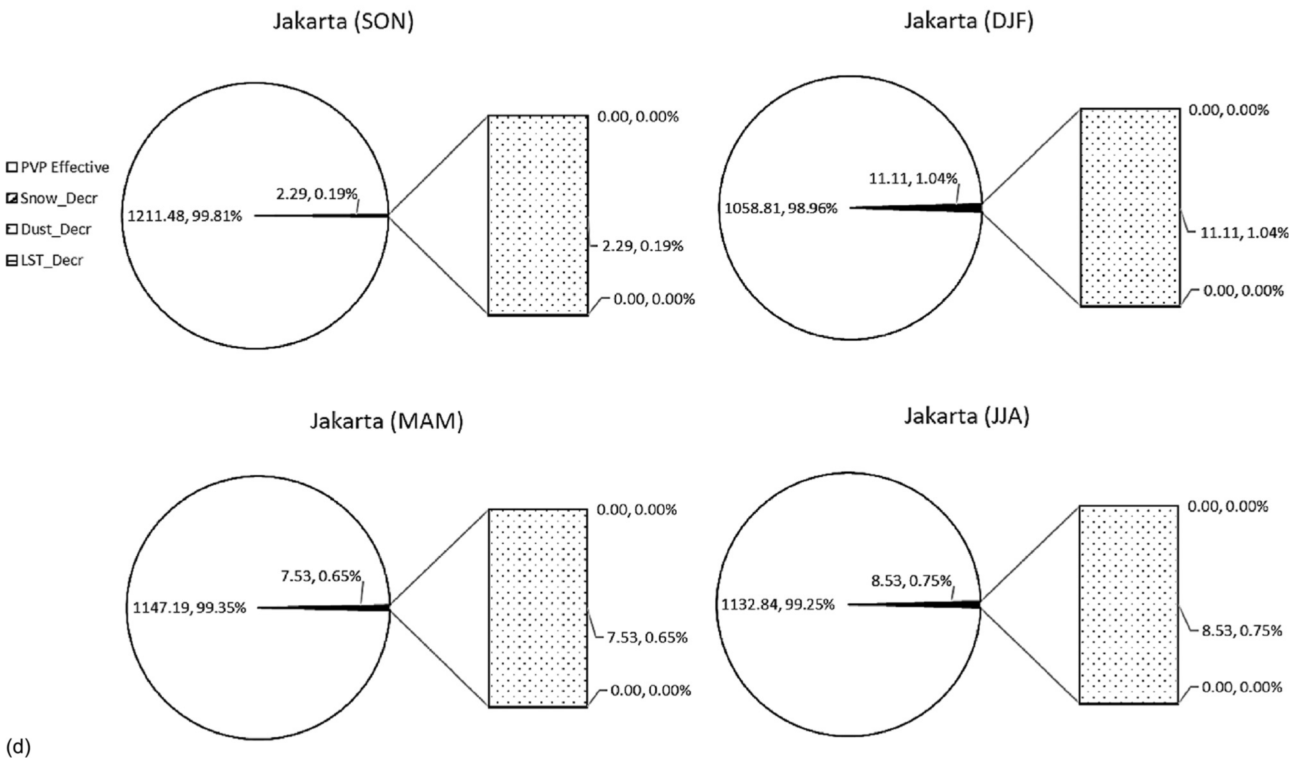

FIG. 9. (*Continued*).

TABLE III. Validation results for solar PV outputs.

	Actual generation (kWh)				Estimated generation (kWh)				PPE (%)[a]			
Solar PV site	MAM	JJA	SON	DJF	MAM	JJA	SON	DJF	MAM	JJA	SON	DJF
Signal Hill	1209	976	1670	1854	750	749	1883	2080	(−) 38.0	(−) 23.3	(+) 12.7	(+) 12.2
Bangkok Soladin	205[b]	63[c]	86[d]	145[e]	269.3	48.8	76.2	160.7	(+) 31.4	(−) 22.5	(−) 11.4	(+) 10.8

[a](−) and (+) denote the model under- and overestimation, respectively.
[b]Number of days with no output: 3.
[c]Number of days with no output: 60.
[d]Number of days with no output: 44.
[e]Number of days with no output: 26.

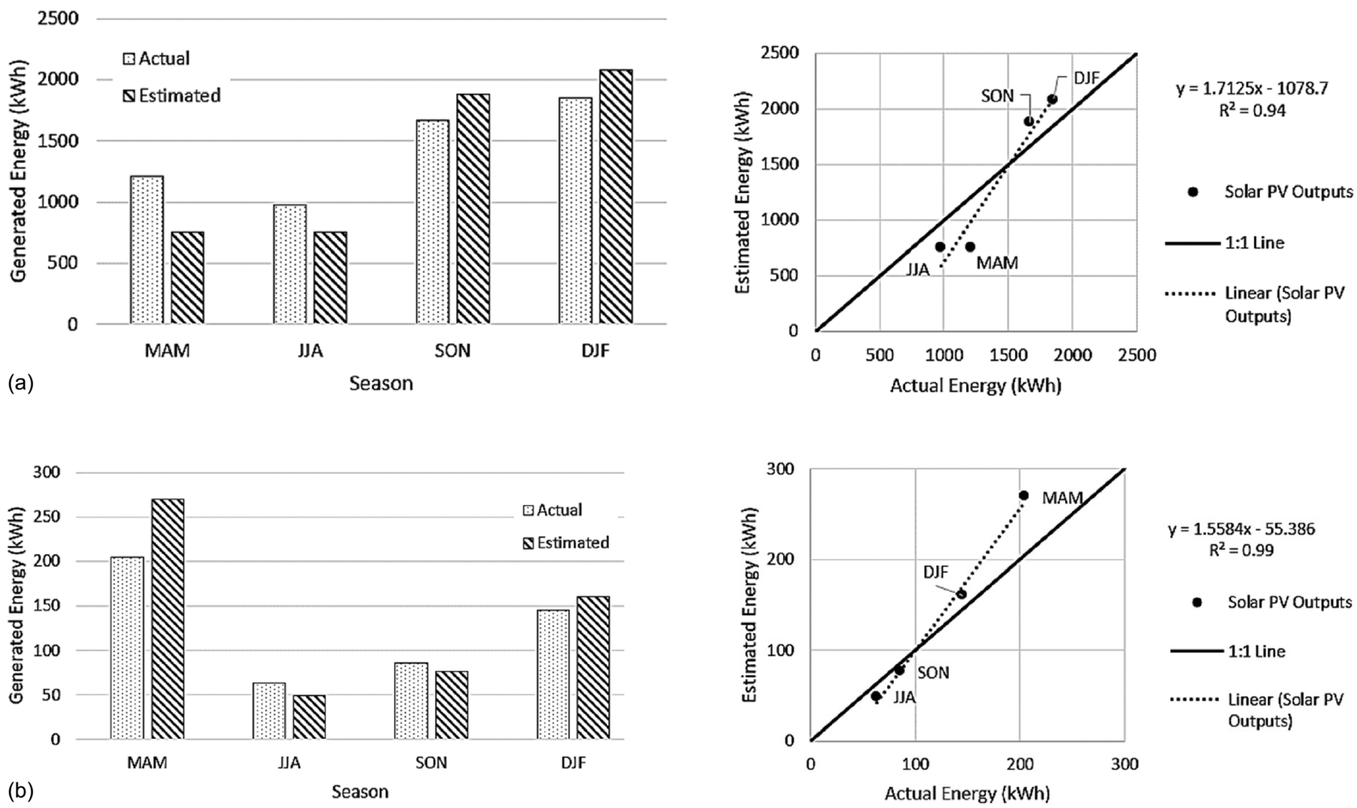

FIG. 10. Comparison of estimated and actual energies in: (a) Signal Hill (SH) and (b) Bangkok Soladin (BS) solar PV installations. It can be seen here that the model underestimates the actual generated energy in JJA and SON seasons at BS and during MAM and JJA for SH but shows promising results in terms of the coefficient of determination.

contributor during MAM; during JJA, there is no significant decrease in P_{PV} (snow's impact is very small at 0.01% and is highly unlikely to be present during this season).

Khabarovsk is consistently affected by snow effects except in JJA when dust is the only contributing factor to the decrease in P_{PV} [Fig. 9(c)]. Finally, in the case of Jakarta [Fig. 9(d)], the only contributing factor is the dust. The case of Jakarta is the same for the other cities in the region with tropical climate. It can be seen in Figs. 9(a)–9(d) that temperature has no effect on the decrease in P_{PV} for the four cities that were examined. In fact, except in extreme cases such as in desert areas, $\Delta\eta_t$ is very negligible for most cities in the Asia Pacific region. As stated previously, this result may change if an actual T_{cell} is computed and reflected in the model instead of LST.

G. Comparison of estimated and actual solar PV outputs

Table III shows the summary of the estimated and actual solar PV outputs for the two installations in Australia and Thailand with their corresponding PPE values. Moreover, Fig. 10 shows the bar charts for Table III. The model underestimated the generated energy MAM and JJA in Signal Hill and JJA and SON seasons in Bangkok Soladin.

The values of PPE range from 10% to 38% with an average value of 22% for Signal Hill and 19% for Bangkok Soladin. This result is close to but better than the reported monthly averaged PPE value (23.6%) by Kim *et al.* (2017) who considered a "practical model" (similar in some respect to our model) for daily prediction of solar PV power generation in South Korea. Moreover, it can be seen in Fig. 10 that there is a good linear correlation between the estimated and actual values as indicated by the very high values (0.94, 0.99) of R^2. The values, however, are quite far from the 1:1 line signifying a very low agreement in the absolute values of the two sets of data. This can be an indication that "rotation" factors should be introduced in the model equations to fit these data points to the 1:1 line. Such a rotation factor can be derived from the solar PV cell efficiency and coefficients of efficiencies both of which were set to fixed values. The conversion from power (MW) to energy (kWh) units can also be a source of error; specifically, it is assumed that sunshine hours are equivalent to the actual number of hours that the solar cells are producing power. The assumption was done since no information on the actual operating hours is available in PVOutput.org.

The model needs more refinement as indicated by unsatisfactory values of PPE. The sources of error can be attributed to the fixed values set for the solar PV cell efficiency (13%) and coefficients of efficiency (0.094, 0.3, and 0.16 for temperature, dust, and snow, respectively). For instance, the published peak efficiencies for the solar cells used in Signal Hill and Bangkok Soladin are 16.9% and 13.1%, respectively. Such an efficiency rate is a possible reason why the estimated values relatively agreed well with the actual values in Bangkok Soladin. Using the satellite-derived LST to estimate the actual solar cell temperature may also introduce significant error since LST itself has limitations due to mixed-pixel issues, complicated surface structures, and topographic effects (Wan, 1999). It is therefore recommended to convert LST to solar panel temperature. Several studies have used explicit equations to derive the operating temperature of a PV module (T_{cell}) from ambient air temperature such as the studies of Alsayed *et al.* (2013) and Gokmen *et al.* (2016), but as far as we know, there has been no study yet that dealt with the derivation of T_{cell} directly from LST. This is therefore a subject of our future work. The binary masking scheme used for dust analysis also has its limitations since AOD can also represent other aerosol particles aside from fine and coarse dusts (e.g., water vapor, etc.). As a future work, we will use the Angstrom coefficient data to determine AOD values which are useful for the analysis of dust effects on solar panels. Finally, the coefficient of efficiency for snow needs to be carefully considered and adjusted if needed since snow types vary for different locations.

IV. CONCLUSIONS

This paper presented a method for incorporating different remote sensing satellite data to investigate the limiting effects of temperature, dust, and snow on the total effective efficiency of the solar PV cells and the corresponding output power potential. The theoretical mean seasonal solar PV power was also derived for the Asia Pacific region with the maximum value at ∼1.9 GW per EPA of 17.5 km^2. The results of this study show a noticeable significant decrease in P_{PV} in Australia for DJF and MAM seasons and a slight decrease during SON. The same can be observed during JJA in China, Mongolia, and Russia.

Different cities are affected differently by temperature, dust, and snow. For Beijing, the major contributor to the decrease in P_{PV} is dust, except in DJF when snow is the major contributor. For Tokyo, the effect varies with the season but mainly dust during MAM. Khabarovsk is consistently affected by snow effects except in JJA when dust is the only contributing factor. Finally, in the case of Jakarta, the only contributing factor is the dust.

The maximum decrease in P_{PV} due to the three meteorological parameters was reached except for snow (the threshold is 16%, but the computed is 12%). It is therefore necessary to investigate this underestimation by considering a more comprehensive analysis of snow dynamics in the region and how it can be incorporated in the model. Although model improvements are still needed, this paper has demonstrated how different remote sensing data can be used to assess the solar PV power potential in a regional scale. The excellent temporal resolution of AHI8 should also be maximized to produce the estimated solar PV power output for every hour at the least. After refining the model, the next step for this study is to include the geomorphological and building/roof type factors in the computation of P_{PV} to consider the tilt and shadow effects.

Globally, it is apparent that there is a strong movement, from government and non-government institutions, pushing for clean energy alternatives. Solar power from PV cells is one of such alternative that is now becoming a more popular choice. This technology is continually progressing to provide a more affordable and more efficient system for the advantage of both the electricity producers and consumers, leading to more stakeholders participating in this industry. Therefore, the output of this study can be useful in planning for small-scale (e.g., solar rooftop) or large-scale solar PV projects (e.g., solar farms) in a solar-rich region of Asia Pacific.

ACKNOWLEDGMENTS

SWR, CLOT, and GSMaP products were supplied by the P-tree System, Japan Aerospace Exploration Agency (JAXA). The authors would like to thank the Hitachi Global Foundation for their support in this research endeavor.

REFERENCES

ADB, *Renewable Energy Developments and Potential in the Greater Mekong Subregion* (Asian Development Bank, Mandaluyong, 2015).

AIIB, *Energy Sector Strategy: Sustainable Energy for Asia* (Asian Infrastructure Investment Bank, Beijing, 2017).

Alsayed, M., Cacciato, M., Scarcella, G., and Scelba, G., "Multicriteria optimal sizing of photovoltaic-wind turbine grid connected systems," IEEE Trans. Energy Convers. **28**, 370–379 (2013).

Australian Government Bureau of Meteorology, http://www.bom.gov.au/watl/sunshine/ for Sunshine: Average Daily Sunshine Hours; accessed 24 April 2018 (2005).

Beattie, N. S., Moir, R. S., Chacko, C., Buffoni, G., Roberts, S. H., and Pearsall, N. M., "Understanding the effects of sand and dust accumulation on photovoltaic modules," Renewable Energy **48**, 448–452 (2012).

Chander, S., Purohit, A., Sharma, A., Nehra Arvind, S. P., and Dhaka, M. S., "A study on photovoltaic parameters of mono-crystalline silicon solar cell with temperature," Energy Rep. **1**, 104–109 (2015).

Chang, A. T. C. and Rango, A., https://nsidc.org/sites/nsidc.org/files/technical-references/amsr_atbd_snow.pdf for Algorithm Theoretical Basis Document (ATBD) for the AMSR-E Snow Water Equivalent Algorithm; accessed 10 September 2018 (2000).

Chen, W. and Sopori, B., "A thin silicon solar cell on glass: Cell design and process physics," in *Electrochemical Society*'99 (NREL, Seattle, 1999), pp. 1–8.

El-Shobokshy, M. S. and Hussein, F. M., "Degradation of photovoltaic cell performance due to dust deposition on its surface," Renewable Energy **3**, 585–590 (1993).

FrouinR., Murakami H., "Estimating photosynthetically available radiation at the ocean surface from adeos-ii global imager data," J. Oceanogr. **63**(3), 493 (2007).

Gokmen, N., Hu, W., Hou, P., Zhe, C., Sera, D., and Spataru, S., "Investigation of wind speed cooling effect on PV panels in windy locations," Renewable Energy **90**, 283–290 (2016).

Goossens, D., Offer, Z. Y., and Zangvil, A., "Wind tunnel experiments and field investigations of eolian dust deposition on photovoltaic solar collectors," Sol. Energy **50**, 75–84 (1993).

Gupta, P., Joiner, J., Vasilkov, A., and Bhartia, P. K., "Top-of-the-atmosphere shortwave flux estimation from satellite observations: An empirical neural network approach applied with data from the A-train constellation," Atmos. Meas. Tech. **9**, 2813–2826 (2016).

Hall, D. K., Riggs, G. A., and Salomonson, V. V., *Algorithm Theoretical Basis Document (ATBD) for the MODIS Snow and Sea Ice-Mapping Algorithms* (NASA, Greenbelt, 2001).

Higurashi, A. and Nakajima, T., "Development of a two-channel aerosol retrieval algorithm on a global scale using NOAA AVHRR," J. Atmos. Sci. **56**, 924–941 (1999).

Jin, M. and Dickinson, R. E., "Land surface skin temperature climatology: Benefitting from the strength of satellite observations," Environ. Res. Lett. **5**, 041002 (2010).

Kim, J.-G., Kim, D.-H., Yoo, W.-S., Lee, J.-Y., and Kim, Y. B., "Daily prediction of solar power generation based on weather forecast information in Korea," IET Renewable Power Gener. **11**(10), 1268–1273 (2017).

Kimber, A., Mitchell, L., Nogradi, S., and Wenger, H., "The effect of soiling on large grid-connected photovoltaic systems in California and the Southwest region of the United States," in *Proceedings of the 2006 IEEE 4th World Conference on Photovoltaic Energy Conference*, Waikoloa (2006), pp. 2391–2395.

Lee, S., Kim, B., Lee, K., Zo, I., Jung, H., and Rim, S., "Retrieval of reflected shortwave radiation at the top of the atmosphere using Himawari-8/AHI data," Remote Sens. **10**(2), 1–25 (2018).

Levy, R. C., Mattoo, S., Munchak, L. A., Remer, L. A., Sayer, A. M., Patadia, F., and Hsu, N. C., "The collection 6 MODIS aerosol products over land and ocean," Atmos. Meas. Tech. **6**, 2989–3034 (2013).

Li, Z., Guo, X., Dixon, P., and He, Y., "Applicability of land surface temperature (LST) estimates from AVHRR satellite image composites in northern Canada," Prairie Perspect. **11**, 119–130 (2008).

Liu, B., Li, K., Niu, D. D., Jin, Y. A., and Liu, Y., "The characteristic analysis of the solar energy photovoltaic power generation system," IOP Conf. Ser.: Mater. Sci. Eng. **164**, 1–6 (2017).

Menes-Rodrìguez, D., Horley, P. P., Gonzàlez-Hernàndez, J., Vorobiev, Y. V., and Gorley, P. N., "Photovoltaic solar cell performance at elevated temperatures," Sol. Energy **78**, 243–250 (2005).

Mildrexler, D. J., Zhao, M., and Running, S. W., "A global comparison between station air temperatures and MODIS land surface temperatures reveals the cooling role of forests," J. Geophys. Res. **116**, G03025, https://doi.org/10.1029/2010JG001486 (2011).

NAIT, *Alternative Energy Program: Solar Photovoltaic Reference Array Report* (Northern Alberta Institute of Technology, Edmonton, 2016).

Okamoto, K., Iguchi, T., Takahashi, N., Iwanami, K., and Ushio, T., "The global satellite mapping of precipitation (GSMaP) project," in 25th IGARSS, Seoul (2005).

Paudyal, B. R. and Shree, R. S., "Dust accumulation effects on efficiency of solar PV modules for off grid purpose: A case study of Kathmandu," Sol. Energy **135**, 103–110 (2016).

Perovich, D. K., "Light reflection and transmission by a temperate snow cover," J. Glaciol. **53**(181), 201–210 (2007).

Principe, J. and Takeuchi, W., "Assessment of solar PV power potential over Asia Pacific region with AHI8," in 26th Institute of Industrial Science (IIS) Forum, Tokyo (2018).

PVOutput.org, https://pvoutput.org/ for PVOutput. PVOutput.org; accessed 23 April 2018.

REN21, *Renewables 2017 Global Status Report* (REN21 Secretariat, Paris, 2017).

Sampaio, P. G. V. and Gonzalez, M. O. A., "Photovoltaic solar energy: Conceptual framework," Renewable Sustainable Energy Rev. **74**, 590–601 (2017).

Sayigh, A. A. M., "Effect of dust on flat plate collectors. Sun, mankind's future source of energy," in *Proceedings of the International Solar Energy Society Congress*, New Delhi (1978), pp. 960–964.

Sims, R. E. H., Schock, R. N., Adegbululgbe, A., Fenhann, J., Konstantinaviciute, I., Moomaw, W., Nimir, H. B., *et al.*, "Energy supply," in *Climate Change* 2007: *Mitigation. Contribution of Working Group III to the Fourth Assessment Report of the Intergovernmental Panel on Climate Change*, edited by B. Metz, O. R. Davidson, P. R. Bosch, R. Dave, and L. A. Meyer (Cambridge University Press, Cambridge, UK/New York, USA, 2007).

Thai Meteorological Department, https://www.tmd.go.th/agromet.php for "Agrometeorology," accessed 24 April 2018 (2014).

The World Bank, https://data.worldbank.org/indicator/EG.USE.ELEC.KH.PC for "Electric power consumption (kWh per capita)," The World Bank Data; accessed 23 April 2018 (2014).

US EIA, https://www.eia.gov/outlooks/ieo/ for "International Energy Outlook 2017," Independent Statistics and Analysis: US Energy Information Administration, accessed 23 March 2018 (2017).

Wan, Z., *MODIS Land-Surface Temperature Algorithm Theoretical Basis Document (LST ATBD)* (Institute for Computational Earth System Science, Santa Barbara, 1999).

Wu, S. and Xiong, C., "Passive cooling technology for photovoltaic panels for domestic houses," Int. J. Low-Carbon Technol. **9**(2), 118–126 (2014).